Fast adiabatic heating and temperature relaxation in near-critical fluids under zero gravity

Marco Bonetti, F. Perrot, Daniel Beysens, Yves Garrabos

Fast Adiabatic Heating and Temperature Relaxation in Near-Critical Fluids Under Zero Gravity[1]

M. Bonetti,[2,3] F. Perrot,[2] D. Beysens,[2] and Y. Garrabos[4]

Heat transport in supercritical CO_2 is studied under microgravity conditions. A large temperature and density ρ region around the critical point is explored (CO_2 cells were filled at critical density $\rho = \rho_c$ and off-critical densities $\rho = \rho_c \pm 0.18\rho_c$). Local heating is obtained by using a small thermistor located in the bulk fluid. Through interferometric observations, a new mechanism of thermalization has been evidenced. Thermal expansion of a warm diffusing boundary layer around the heating thermistor is responsible for rapid adiabatic heating of the bulk fluid through the emission of pressure waves at the border. The scaled thickness of the thermal boundary layer follows a power law. When the heat flow stops, the bulk adiabatic heating instantaneously vanishes and the temperature relaxation inside the thermal boundary layer follows locally a diffusive process.

KEY WORDS: CO_2; critical-point phenomena; thermal diffusion.

1. INTRODUCTION

Recently, heat thermal equilibration in pure fluids near their critical point has received much attention [1–8]. In such fluids, isothermal compressibility diverges near the critical temperature T_c and pressure waves strongly contribute to the heat transport. This mechanism, coined the piston effect (PE), has been detailed in numerical simulations [9]. When a wall of a cell containing a supercritical fluid is instantaneously heated, a thermal boundary layer expands and acts as a piston, thereby generating acoustic

[1] Paper presented at the Twelfth Symposium on Thermophysical Properties, June 19–24, 1994, Boulder, Colorado, U.S.A.

[2] Service de Physique de l'État Condensé, Commissariat à l'Énergie Atomique, Centre d'Études de Saclay, Orme des Merisiers, F-91191 Gif-sur-Yvette Cedex, France.

[3] To whom correspondence should be addressed.

[4] Laboratoire de Chimie du Solide, Centre National de la Recherche Scientifique, Université de Bordeaux I, 351 cours de la Libération, F-33405 Talence Cedex, France.

waves which propagate in the bulk. Through the propagation of these compression waves, the bulk fluid experiences an adiabatic pressure increase. Adiabatic thermal conversion of the pressure waves gives a spatially uniform temperature increase in the bulk fluid on a time scale comparable to a few acoustics times t_s ($t_s = L/c$, where L is a typical dimension of the cell and c is the speed of sound at the cell temperature). This brings about a *speeding-up* of the heat transport, in contrast to the *critical slowing-down* observed in purely diffusive incompressible fluids. As first introduced by Onuki and Ferrell [10], the typical time of the heat transport in the thermal boundary layer is $t_c = t_D/(\gamma - 1)^2$. Here $t_D = L^2/D_t$ is the diffusive time, where D_t is the thermal diffusivity and $\gamma = c_p/c_v$ is the ratio of the specific heats c_p and c_v at constant pressure and volume, respectively. The time t_c can be understood to be the typical diffusing time for the heat transport through a thermal boundary layer of thickness $\delta = L/(\gamma - 1)$ into the fluid bulk. Near T_c, γ diverges and therefore δ and t_c go to 0.

We report here quantitative interferometric experiments performed under microgravity conditions when PE is active. Microgravity is essential to avoid convection, which destabilizes the thermal boundary layer around the heating point. The evolution of the thermal boundary layer and the corresponding thermal response of the bulk fluid are investigated in a CO_2 cell when heat is continously released. Different values of density and temperature have been studied. The major finding is that the bulk fluid is rapidly heated on a time scale t_s as the thermal boundary layer expands. The layer thickness is seen to scale with δ and t_c. Temperature relaxation at the heating point is also measured. This is obtained after a short heat pulse, of time duration of order 0.5 s. The temperature relaxation inside the warm thermal boundary layer follows locally a diffusive process since the PE is no longer active when the heat flow is stopped.

2. EXPERIMENT

Sample cells are filled with CO_2 (Air Liquide; purity >99.998%) at a critical density $\rho_c = 467.9\ \mathrm{kg \cdot m^{-3}}$ and at two off-critical densities $\rho = \rho_c \pm 0.18\rho_c$, with an accuracy better than 0.1%. The critical temperature and pressure are 304.14 K and 7.37 MPa. These high-pressure cells are made of copper beryllium and are cylindrically shaped with an inner diameter $\Phi = 11.6$ mm and thickness $e = 6.8$ mm. Two sapphire windows at each end of the cylinder allow interferometric observations. Each cell is positioned in one arm of a Twymann–Green interferometer which is housed on the top of a unit (sample cell unit; SCU) made of electrolytical copper. The SCU is a cylinder of 60-mm outer diameter and 115-mm length whose temperature can be finely controlled to within 50 μK over several hours.

Due to the high thermal diffusivity of copper, the thermal time constant of the SCU (≈ 2 s) is comparable to that of the fluid cell body (from 2 to 20 s). Two identical and nearly spherical thermistors are located in the fluid cell at an equal distance from the sapphire windows. Their diameter is 0.9 mm, with a time constant of 100 ms. The distance between their centers ($L_1 = 4.6$ mm) is comparable to the distance $L_2 = 3.5$ mm between the thermistor center and the cell walls and to the half-distance between the inner windows ($e/2 = 3.4$ mm). Only one thermistor (referenced Th1) is used to heat the fluid for a given period of time. Both thermistors can measure the temperature of the fluid only when the heating is off. Thermistor Th2 measures the temperature of the bulk fluid outside the warm thermal boundary layer. In this way, its temperature depends mainly on the heat transfer by pressure waves due to PE. Thermistor Th1 delivers

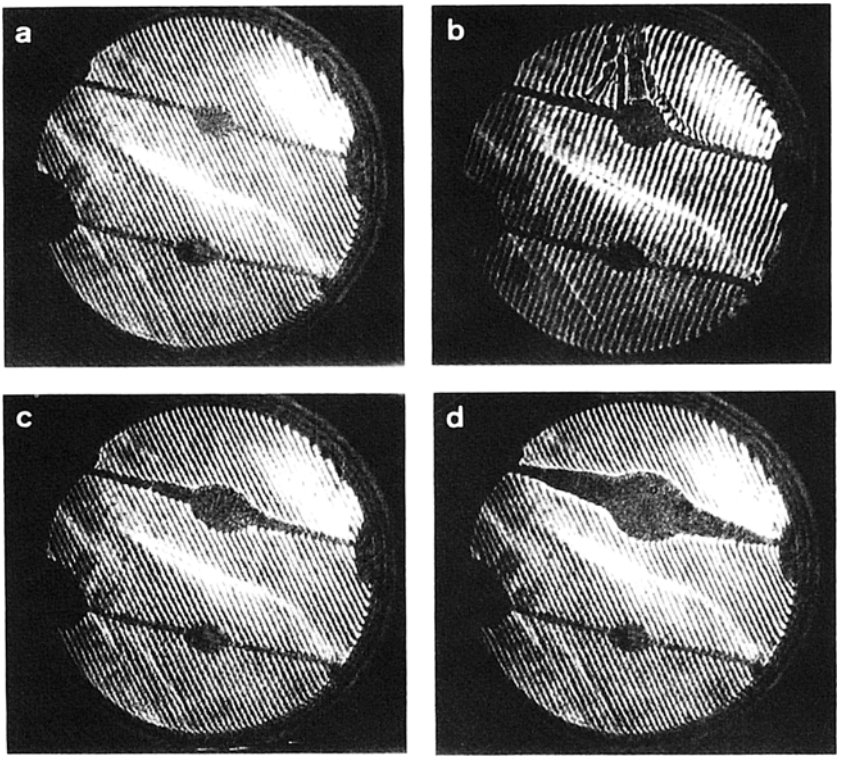

Fig. 1. Thermal layer around a heating thermistor (CO_2 at $\rho = \rho_c$). (a) Before heating. View of the cell (11.6-mm diameter) with both thermistors (the two spheres). The bright and dark lines are interference fringes. (b) Experiment under Earth gravity ($T = T_c + 16$ K), 400 ms after heating has started. (c) Experiments under microgravity ($T = T_c + 16.8$ K), $t = 480$ ms after heating has started, (d) Same as c but at $t = 2$ s.

into the fluid a quantity of heat which depends on the thermistor temperature through its calibration curve. In these experiments, the typical delivered power ranges between 12.2 and 80 mW. The bulk temperature relaxation process is part of a separate analysis [11].

At equilibrium and with a homogeneous density, straight interference fringes were set in the view field (≈ 40 fringes in the pattern; Fig. 1a). Density changes in the bulk or at the cells walls result in a refractive index variation and fringes are shifted and/or distorted. Density and refractive index are related through the Lorentz–Lorenz relation [12]. The interference pattern is recorded by a CCD videocamera at 25 Hz.

The maximum temperature acquisition rate is 25 Hz. To reduce the thermal perturbation near T_c in the measuring mode (dissipated power, $3\,\mu$W at $T = T_c + 16$ K), temperature is sampled each 2 s when needed.

3. INTERFEROMETRIC OBSERVATIONS

3.1. Continuous Heating

On Earth, a convective plume settles, after a few milliseconds, in the fluid and destroys the thermal boundary layer around the heating thermistors Th1 (Fig. 1b). In contrast, under microgravity conditions (g-jitter $< 10^{-4}$), a nearly spherical shaped thermal boundary layer forms around Th1 (Figs. 1c and d). This layer appears as a black region where the fringes are not visible. Outside this region, the fringes in the bulk region are not distorted. This means that the fluid density remains homogeneous. Simultaneously, one observes a displacement of the whole fringe pattern in the bulk region. This instantaneous translation of the fringe pattern corresponds to a spatially uniform density change throughout the bulk fluid. This is achieved through propagating compression waves which travel back and forth in the cell and whose characteristic time is related to the acoustic time t_s.

3.2. Pulse Heating: Temperature Relaxation of the Boundary Layer

Figures 2a and b show the relaxation mechanism at $T_c + 15.9$ K when the heating has been stopped. Fringes form at the border of the thermal layer with a fringe spacing which increases with time. Figure 2a is taken at $t = 10.5$ s after the end of a 480-ms heat pulse, and Fig. 2b at $t = 13.5$ s. The same fringe pattern evolution is observed near T_c but the relaxation mechanism is much slower. This suggests that the thermal relaxation in the boundary layer is a diffusing process. In the following, we see that temperature relaxation measurements confirm this analysis.

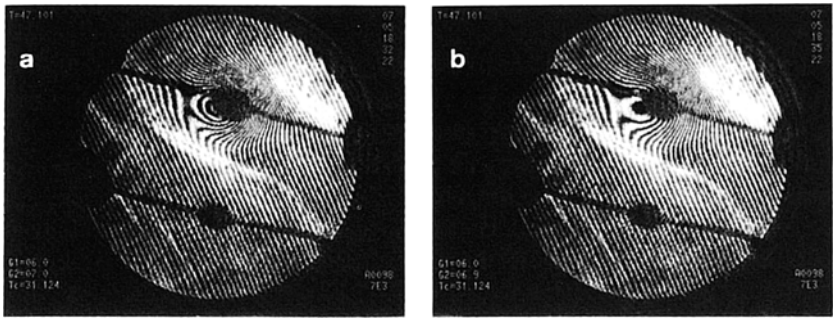

Fig. 2. Thermal relaxation of the boundary layer (CO_2 at $\rho = \rho_c$) after a short heating pulse ($\Delta t = 480$ ms, $T = T_c + 15.9$ K). (a) At $t = 10.5$ s after the end of heating, (b) At $t = 13.5$ s. Notice the appearance of curved fringes in the boundary layer and the increasing of the fringe spacing in time.

4. DISCUSSION

After a fast temperature increase at the wall, the bulk temperature should increase within the characteristic time t_c. The thickness of the thermal boundary layer e_b should be of the order of δ as defined previously. In our experiment the layer thickness $e_b = r_b - r_{th}$ (with r_b the external radius of the layer and r_{th} the radius of the thermistance) scales with δ $\{\delta = (e/2)[1/(\gamma - 1)]\}$ when expressed versus the reduced time t/t_c $\{t_c = (e^2/4)(1/D_t)[1/(\gamma - 1)^2]\}$. Figure 3 shows a log–log plot of the reduced thickness $e^* = e_b/\delta$ versus the reduced time $t^* = t/t_c$ for $\rho = \rho_c$ and for $\rho = \rho_c \pm 0.18\rho_c$. All data obey a power law $e^* = At^{*0.65}$, where $A \simeq 5$, which is to be compared with the value $A = 1.15$ given by Onuki et al. [10] for the 1-D geometry. Note that scaling holds for a thickness e_b as large as 1000δ and is valid in the supercritical region. We also report a calculation of the evolution of a purely diffusive layer around a heating sphere in an infinite incompressible medium with constant diffusivity. The same power law holds with the same exponent. Note that the exponent 0.65 corresponds to a transient behavior. The classical exponent 0.5 is reached later, as observed in our simulation. For example, at critical density $\rho = \rho_c$ and $T = T_c + 16.8$ K, an exponent 0.65 is observed up to ≈ 60 s and decreases for longer times.

The bulk density evolution is measured by means of the fringe shift. The relative density variation $\Delta\rho/\rho$ per fringe shift is 0.04%. We have counted the number of fringes which cross a reference line. The local density increase in a fluid of mass M, receiving an energy amount E, due to

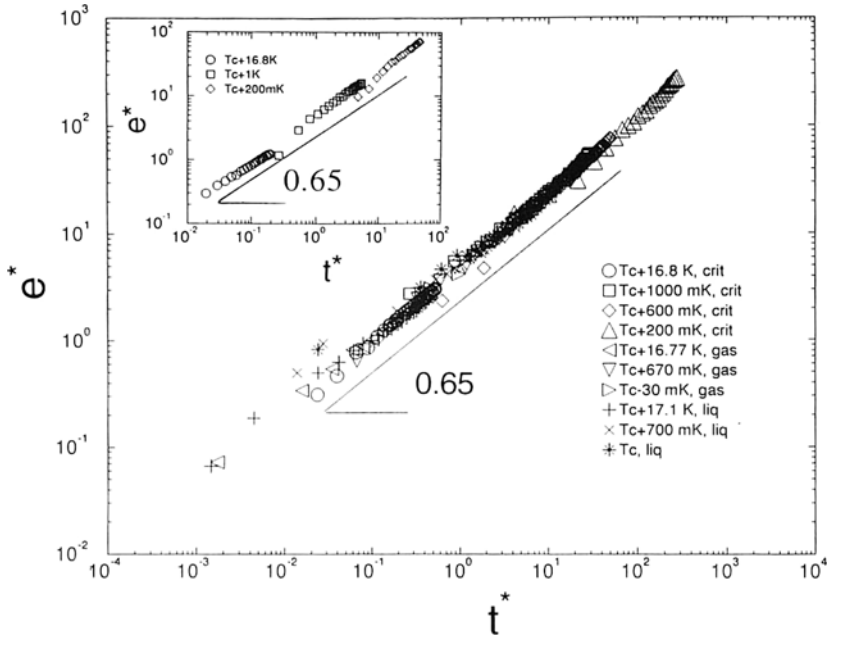

Fig. 3. Thermal layer expansion during continuous heating: reduced layer thickness e^* vs reduced time t^* (see text) at various CO_2 densities and temperatures. Inset: Calculation of the evolution of the thermal layer thickness in a purely diffusive process at $\rho = \rho_c$.

adiabatic heating, is given by $\delta\rho = (\partial\rho/\partial T)_p [1/(\gamma - 1)\, c_v](E/M) \equiv R(E/M)$. In Fig. 4, we show the density variations in the bulk normalized to R ($\delta\rho^* = \delta\rho/R$). All curves collapse on one single curve for $t < 15$ s. The time variation of $\delta\rho^*$ is not simple to analyze because of the thermistor self-heating phenomenon, which increases the heating power with time.

A simulation of the fringes pattern shows a striking similarity to the fringe distortion observed in Fig. 2 in the temperature relaxation mode. Figure 5a shows a computed interferometric fringe pattern produced by a 2-D Gaussian distributed inhomogeneity of the refractive index in a medium of constant index. The refractive index value of the central peak taken with respect to the bulk index is 10^{-4}. We observe the appearance of a circular region with a well-defined border. In this region, fringes are distorted and the fringe spacing is smaller than in the bulk region. By decreasing the peak value of the refractive index, the fringe spacing enlarges in the inhomogeneous region while the fringes become less bent. Figure 5b shows the fringes pattern computed for a refractive index peak value of 0.5×10^{-4}. From these simulations, we infer that the black region around

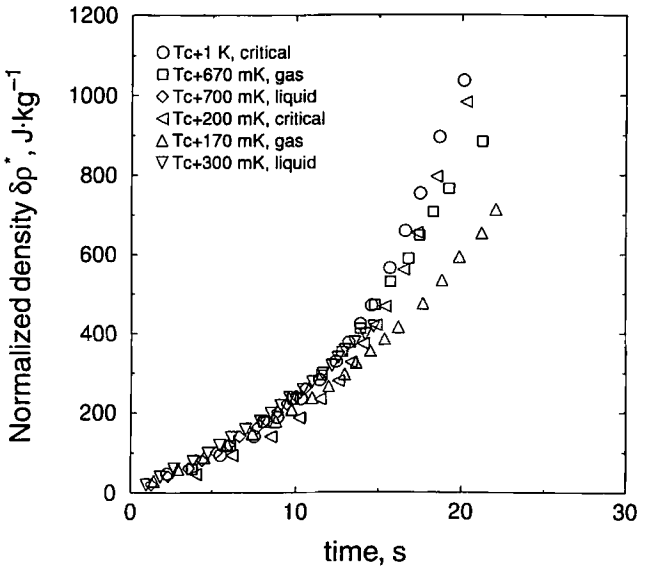

Fig. 4. Normalized density increase $\delta\rho^*$ vs time (see text) at various CO_2 densities and cell temperatures.

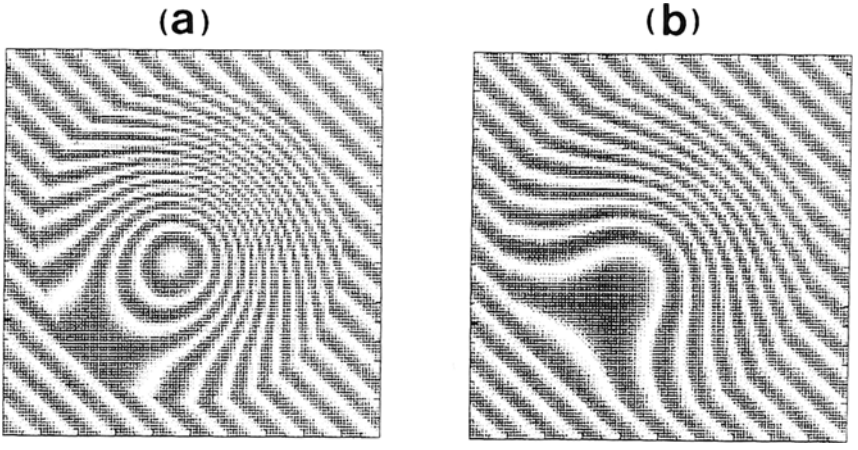

Fig. 5. Simulation of the interference fringe pattern: effect of a refractive index inhomogeneity in a uniform refractive index medium (see text). Notice the same distortion of the fringe pattern as in the experimental case in Fig. 2.

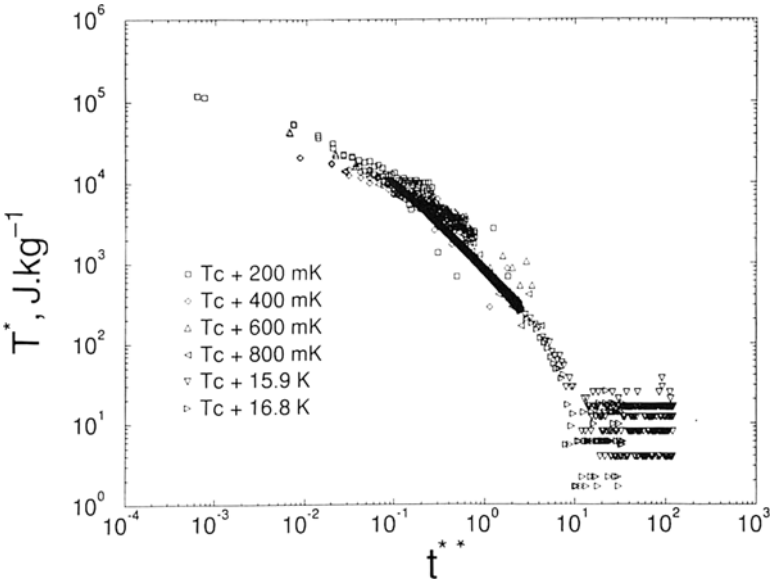

Fig. 6. Reduced temperature relaxation $T^* = Tc_p$ after a short heat pulse ($\Delta t = 480$ ms) of the thermal boundary layer for various cell temperatures, at CO_2 critical density, vs reduced time $t^{**} = t/t_D$.

the heating point is a region with high refractive index gradients—and hence density gradients—where the fringe visibility is strongly reduced. We have also deduced that the border of the thermal layer corresponds to a density inhomogeneity of order 1%.

The temperature relaxation of the heating thermistor has been measured after a heat pulse of duration 480 ms. Figure 6 shows a log–log plot of the reduced temperature T^* as a function of the reduced time t^{**} at different cell temperatures from $T_c + 16.8$ K down to 200 mK and for the critical density. Time is expressed as units of the diffusing time $t_D = (e_{b,max})^2/D_t$, where $e_{b,max}$ is the largest boundary layer thickness measured after the heating has stopped. Temperature is multiplied by c_p, thus defining a reduced temperature T^* with dimension in $J \cdot kg^{-1}$, which represents the energy density contained in the thermal boundary layer. All data collapse on a single curve. This confirms that the heat transport—in the relaxation mode—follows locally a diffusive process.

5. CONCLUSION

We have shown that when a permanent heat flow is released in a compressible fluid, an expandable thermal layer forms at the heating point.

The thickness of the thermal layer follows a power law under proper scaled time (characteristic PE time, t_c) and scaled space (characteristic boundary layer thickness, δ). A uniform density—hence temperature—increase in the bulk is observed corresponding to pressure waves propagating in the fluid. This is the signature of the piston effect.

When the heat flow is stopped, we have also observed that the temperature at the core of the thermal layer relaxes following a diffusive process.

ACKNOWLEDGMENTS

This work was supported by the CNES (Centre National d'Études Spatiales). The experiments were performed in 1992 in the laboratory ALICE [14] onboard the orbital station MIR (ANTARES mission). We are particularly indebted to P. Koutsikidès and J. M. Laherrère from the ALICE project.

REFERENCES

1. J. V. Sengers, in *Critical Phenomena, Proc. Int. School "Enrico Fermi,"* Course LI, M. S. Green, ed. (Academic Press, New York, 1971), p. 445.
2. A. M. Radhwan and D. R. Kassoy, *J. Eng. Math.* **18**:133 (1984).
3. K. Nitsche and J. Straub, *Naturwissenschaffen* **73**:370 (1986).
4. R. P. Behringer, A. Onuki, and H. Meyer, *J. Low Temp. Phys.* **81**:71 (1990).
5. H. Boukari, M. E. Briggs, J. N. Shaumeyer, and R. W. Gammon, *Phys. Rev. Lett.* **65**:2654 (1990).
6. H. Klein, G. Schmitz, and D. Woermann, *Phys. Rev. A* **43**:4562 (1991).
7. P. Guenoun, B. Khalil, D. Beysens, Y. Garrabos, F. Kammoun, B. Le Neindre, and B. Zappoli, *Phys. Rev. E* **47**:1531 (1993).
8. M. Bonetti, F. Perrot, D. Beysens, and Y. Garrabos, *Phys. Rev. E* **49**:4779 (1994).
9. B. Zappoli, D. Bailly, Y. Garrabos, B. Le Neindre, P. Guenoun, and D. Beysens, *Phys. Rev. A* **41**:2264 (1990).
10. A. Onuki and R. A. Ferrell, *Physica A* **164**:245 (1990); A. Onuki, H. Hao, and R. A. Ferrell, *Phys. Rev. A* **41**:2256 (1990).
11. Y. Garrabos, M. Bonetti, D. Beysens, F. Perrot, T. Frohlich, P. Carlès, and B. Zappoli, (submitted).
12. M. Born and E. Wolf, *Principles of Optics*, 6th ed. (Pergamon Press, New-York, 1980).
13. H. S. Carslaw and J. C. Jaeger, *Conduction of Heat in Solids*, 2nd ed. (Oxford University Press, London, 1959).
14. J.-M. Laherrère and P. Koutsikidès, *Acta Astronaut.* **29**(10/11):861 (1993).